View metadata, citation and similar papers at core.ac.uk

brought to you by CORE

provided by Elsevier - Publisher Connector

Virology 377 (2008) 319–329

Contents lists available at ScienceDirect

Virology

journal homepage: www.elsevier.com/locate/yviro

Expression profile of interferon stimulated genes in central nervous system of mice infected with dengue virus Type-1

Juliano Bordignon [a,b,1], Christian M. Probst [a,b,1], Ana Luiza P. Mosimann [a,b], Daniela P. Pavoni [a,b], Vanessa Stella [a,b], Gregory A. Buck [c], Nusara Satproedprai [c], Paul Fawcett [d], Sílvio M. Zanata [e], Lucia de Noronha [f], Marco A. Krieger [a,b], Claudia N. Duarte dos Santos [a,b,*]

[a] Instituto de Biologia Molecular do Paraná (IBMP), Rua Prof Algacyr Munhoz Máder 3775, 81350-010, Curitiba, Paraná, Brazil
[b] Instituto Carlos Chagas (ICC)/FIOCRUZ. Rua Prof Algacyr Munhoz Máder 3775, 81350-010, Curitiba, Paraná, Brazil
[c] Center for the Study of Biological Complexity, West Cary Street, 1000, 23284-2030 from Virginia Commonwealth University, Richmond, Virginia, USA
[d] Department of Internal Medicine, East Broad Street, 1001, 23298-0663 from Virginia Commonwealth University, Richmond, Virginia, USA
[e] Departamento de Patologia Básica/Universidade Federal do Paraná, Rua Coronel Francisco H dos Santos, Jardim das Américas, 81531-990, Curitiba, Paraná, Brazil
[f] Laboratório de Patologia Experimental/Pontifícia Universidade Católica do Paraná, Rua Imaculada Conceição, 1155, 80215-901, Prado Velho, Curitiba, Paraná, Brazil

ARTICLE INFO

Article history:
Received 7 February 2008
Returned to author for revision
3 March 2008
Accepted 24 April 2008

Keywords:
Dengue virus
Interferon
Microarray
Mice
Central nervous system

ABSTRACT

Dengue virus (DENV) infection can cause a self-limiting disease (dengue fever) or a more severe clinical presentation known as dengue hemorrhagic fever (DHF)/dengue shock syndrome (DSS). Furthermore, data from recent dengue epidemics in Brazil indicate that the neurological manifestations are becoming more prevalent. However, the neuropathogenesis of dengue are not well understood. The balance between viral replication efficiency and innate immunity — in opposition during the early stages of infection — determines the clinical outcome of DENV infection. In this study, we investigated the effects of DENV infection on the transcription profile of the central nervous system (CNS) of mice. We observed in infected mice the up-regulation of 151 genes possibly involved in neuropathogenesis of dengue. Conversely, they may have a protective effect. Ingenuity Systems software analysis demonstrated, that the main pathways modulated by DENV infection in the mouse CNS are involved in interferon signaling and antigen presentation.

© 2008 Elsevier Inc. All rights reserved.

Introduction

Dengue is a mosquito-borne flavivirosis caused by four dengue virus serotypes (DENV1, 2, 3 and 4). It is epidemic in tropical and subtropical regions around the world. DENV infections have become a major international public health concern (Gubler, 1997) in recent years. The World Health Organization (WHO) estimates that at least 2.5 billion people are at risk of contracting dengue and the number of infections worldwide may reach 10 million cases per year (Clyde et al., 2006; WHO, 2002). In Brazil, more than 4 million cases of dengue have been recorded since its re-introduction in 1986 (SVS, 2007).

DENV1, 2, 3 and 4 are from the *Flaviviridae* family. Infection with any of these serotypes can cause dengue fever (DF), a self-limiting disease, or dengue hemorrhagic fever/dengue shock syndrome (DHF/DSS), characterized by vascular permeability and abnormal homeostasis (Halstead, 1988). The mechanisms involved in the progression of a certain proportion of cases to severe disease are not completely understood. DHF/DSS may develop as a result of immune sensitization from prior DENV infection (Halstead and O'Rourke, 1977) or possibly through a cytokine-mediated process of plasma leakage, involving interactions between DENV-infected monocytes/macrophages and memory $CD4^+$ and $CD8^+$ DENV-reactive T cells (Pang et al., 2007; Rothman, 2003; Kurane et al., 1990). Recently, Luplertlop et al. (2006) demonstrated that immature dendritic cells infected with DENV2 overproduce a metalloproteinase 9 and 2 (MMP-9 and MMP-2) in a viral dose-dependent manner. MMP-9 and MMP-2 seem to enhance endothelial permeability, by reducing the expression levels of genes encoding platelet endothelial adhesion molecule 1 (PECAM-1) and vascular endothelium (VE)-cadherin cell adhesion molecules, causing the redistribution of F-actin fibers. Thus, production of these proteinases could contribute to the pathogenesis of DHF.

During epidemic peaks, approximately 80% of dengue cases seem to be asymptomatic or produce mild disease symptoms, suggesting that innate immunity can neutralize the DENV infection (Navarro-Sánchez et al., 2005). DENV replication during the early stages of infection may determine clinical outcomes; thus, it is important to understand the impact of dengue virus infection on the host innate immunity. Until recently, innate immunity was considered to be a semi-obsolescent hold-over from invertebrate immunity that has been largely superseded by the acquired (adaptive) immune system of vertebrates.

* Corresponding author. Fax: +55 41 33163267.
E-mail address: clsantos@tecpar.br (C.N. Duarte dos Santos).
[1] Juliano Bordignon and Christian M. Probst contributed equally to this study.

0042-6822/$ – see front matter © 2008 Elsevier Inc. All rights reserved.
doi:10.1016/j.virol.2008.04.033

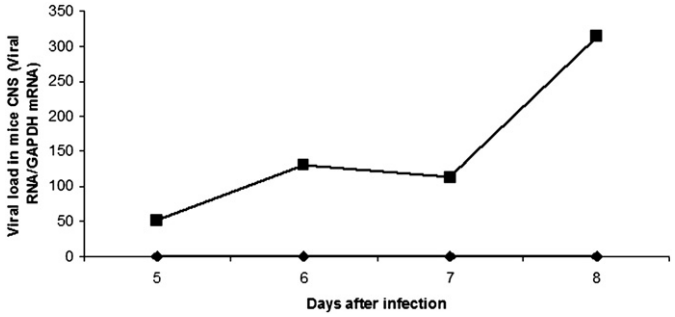

Fig. 1. Viral load in mouse brain infected with DENV1. Viral load in the CNS of Swiss mice infected with 8000 C6/36 ffu of DENV1 at 5, 6, 7 and 8 days post-infection (dpi). Levels of viral RNA were normalized using GAPDH mRNA. Mock-infected animals (♦) and FGA/89 infected animals (■).

However, it has become apparent that the innate and acquired immune systems cooperate to create an effective anti-microbial immune response (Fearon, 1999). Additionally, innate immunity is important in shaping the adaptive immune response, and has anti-cancer and immunomodulatory activities (Delhaye et al., 2006).

Early activation of natural killer (NK) cells and interferon-dependent immunity (IFN) may be also important in limiting viral replication during the first stages of DENV infection. Thus, the varying ability of DENV strains to overcome the innate immunity may underlie differences observed in their virulence (Navarro-Sánchez et al., 2005; Shresta et al., 2004). Additionally, genetic polymorphisms in IFN-stimulated genes (ISGs) may account for differences between hosts in the capacity to fight against infection (Knapp et al., 2003). Currently there is no specific therapy or vaccine available for DF or DHF/DSS. Therapies targeting the innate immunity may be of interest in addressing this issue (Rothman, 2004).

The aim of this study was to evaluate modulation of gene expression by DENV1 infection in the central nervous system (CNS) of mice. Our findings demonstrate a strong induction of ISG mRNAs with known antiviral activity despite the fact that we did not detect the production of cytokine transcripts, including IL-8, IL-6, TNF-α, and IFN-α, β, and g using microarray technology. The pattern of the innate immunity response in DENV infections may provide new insight into the immunopathogenesis of dengue and open up new possibilities for dengue treatment based on immunomodulation.

Results

DENV replication in mice CNS

We previously demonstrated a maximum viral replication activity for FGA/89 in the mouse central nervous system at 9 dpi (Bordignon et al., 2007). We analyzed the transcription profile of the CNS in mice at 5, 6, 7 and 8 dpi — before maximum replication activity was reached — to study the early stages of DENV infection. Viral replication activity was 6.1-fold higher on dpi 8 than that on dpi 5 in animals infected with DENV1 FGA/89 (51.3 viral RNA/GAPDH mRNA on day 5; 313.7 viral RNA/GAPDH mRNA on 8 dpi) (Fig. 1).

We previously demonstrated that DENV replicates efficiently and produces viable viral particles in murine neuronal primary cell culture (Bordignon et al., 2007). However, DENV replication in neuronal cells in man is a controversial issue (Clyde et al., 2006). We performed immunohistochemical analyses of brain sections from infected animals to determine the main cellular target for viral replication in the mouse central nervous system (Fig. 2). Analyses of the temporal cortex showed that meningeal cells and the acellular layer (rich in axons and dendrites from neuronal cells and processes from glial cells) were not infected by DENV1. In contrast, the subsequent layer in the

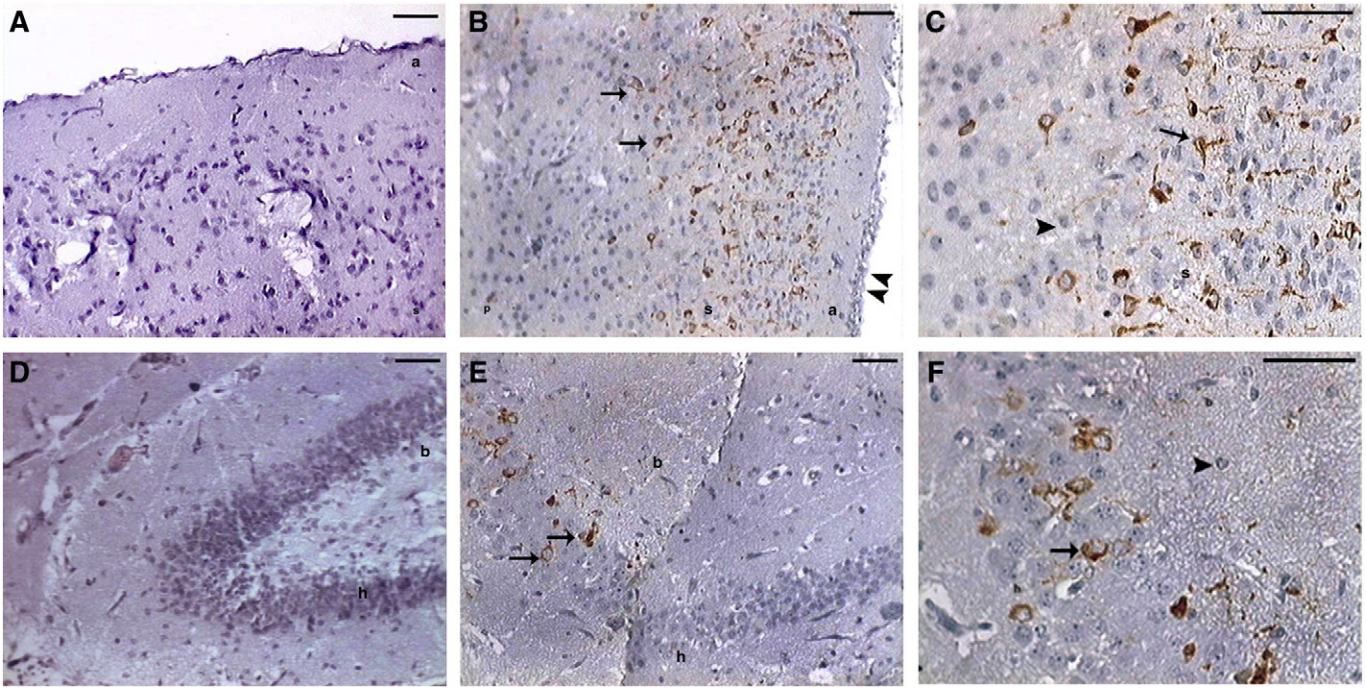

Fig. 2. Immunohistochemical analysis showing DENV1 antigen in brain sections from mock-infected and DENV1-infected Swiss mice at 10 dpi. Panel A and D: Sections of the neuronal cortex and hippocampus, respectively, of mock-infected animals. Panel B: Section of the temporal cortex of DENV1-infected mouse showing absence of meningeal cells (arrow head), absence of antigen-positive cells in the acellular layer (a) (rich in axons and dendrites from neuronal cells and processes of glial cells), and presence of numerous antigen-positive cells (black arrows) in the sequential layer (s), which is composed of temporal neuronal cells. Antigen-positive cells were also not observed in deeper layers (p) of the temporal cortex. Panel C: Enlargement of the sequential layer of the temporal cortex section shown in panel B revealing the DENV1-infected neuronal cells (black arrow) and non-infected astrocytes (arrow head). Panel E: Section of the hippocampus showing some DENV1-antigen-positive cells (black arrows) in the region of hipocampal neurons (h). Panel F: Enlargement of a portion of the section of the hippocampus viewed in panel E, showing antigen-positive hippocampus neuronal cells (black arrow) and non-infected astrocytes (arrow head). Sections were prepared and stained as described in the methods, and images were obtained using an Olympus BX 50 with Image-Pro® Plus software version 4.5 (Maryland). Scale bars are 50 μm.

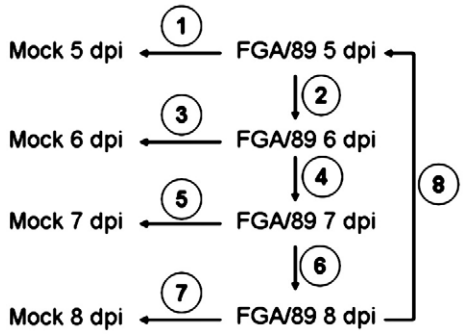

Fig. 3. Microarray experimental design. Numbers 1–8 represent the number of hybridization experiments performed to analyze and compare the gene expression profiles from DENV1-infected mice mock-infected animals. Arrows indicate staining with Cy3 to Cy5 (Cy3 → Cy5).

neuronal cortex contained numerous DENV antigen-positive cells, particularly in the temporal neuronal cell layers (Fig. 2B). We also observed DENV antigen in neuronal cells in the hippocampus, but no viral antigen was detected in white matter using the 4G2 monoclonal antibody (Fig. 2E). Despite our inability to detect viral antigen in astrocytes and oligodendrocytes in the temporal cortex, we cannot exclude the possibility that these cells are targets for DENV1 replication in the mouse CNS (Fig. 2).

Host transcription profile after dengue virus replication

The microarray used in this study encompasses the whole mouse genome, and the hybridizations performed are depicted in Fig. 3. Data from DENV1- and mock-infected animals were compared at each time point as described above, and 151 genes were thus selected (Table 2). Overall, the largest difference in transcription levels between the mock and DENV-infected groups was detected at 8 days post-infection, corresponding to the time of maximum viral replication activity (313.7 viral mRNA/GAPDH mRNA). Thus, gene modulation seems to correlate with viral replication.

Major pathways modulated by DENV infection in the mouse CNS

We determined the major gene induction pathways involved in the response to DENV1 infection of the mouse CNS, by analyzing the 151 selected genes with Ingenuity® Systems software. We found that the main pathways modulated during the infection are those related to the immune response; for example, IFN signaling and antigen presentation (Fig. 4) had the lowest *p*-values (8.96×10^{-16} and 9.19×10^{-14}, respectively). Genes for a number of transcription factors, including signal transducer and activator of transcription 1 and 2 (*Stat1* and *Stat2*), IFN-dependent positive acting transcription factor 3 (*Isgf3g* or *Irf9*) and the IFN regulatory factors 1 and 7 (*Irf1* and *Irf7*), were up-regulated in DENV1-infected mice, demonstrating activation of the IFN-signaling pathway in mice CNS.

Most of the up-regulated genes from the IFN-signaling pathway were ISGs. ISGs encode proteins with antiviral activity; for example, the 2′–5′ oligoadenylate synthetase gene family (*Oas1b, Oas1g, Oasl1, Oasl2, Oas1a* and *Oas2*) which is involved in conferring resistance to West Nile virus (WNV) infection (Kajaste-Rudnitski et al., 2006). Another family of ISG genes that were up-regulated (3.2–49.2 fold) encode IFN-induced proteins with tetratricopeptide repeats (TPR motifs), known as the P56 protein family (Ifit1, 2 and 3) (Table 2; Fig. 5). The TPR motif is a degenerate, 34-amino acid protein–protein interaction module found in multiple copies in a number of functionally distinct proteins that facilitate specific interactions with partner proteins (Blatch and Lassle, 1999; D'Andrea and Regan, 2003; Lamb et al., 1995). Interaction of P56 with one such target, the translation initiation factor 3 (eIF3), leads to translation inhibition (Sarkar et al., 2005). A third major group of ISG genes stimulated in infected mice encodes the IFN-inducible double-stranded RNA-dependent protein kinase (*Prkr* or *Eif2ak2*) family. These proteins phosphorylate the eukaryotic translation factor eIF2α, arresting protein synthesis (Meurs et al., 1992).

Other IFN-stimulated genes represented in CNS of infected mice are those involved in antigen processing and presentation — immunoproteasome assembly (*Psmb8* and *Psmb9*), transportation of processed antigen to endoplasmic reticulum (*Tap1* and *Tap2*) and presentation of antigen on the cell surface by major histocompatibility molecules (MHC) class I (*H2-T9, H2-T10, H2-T22, H2-T23, H2-K1, H2-Q2, H2-Q6, H2-Q7, H2-Q8,* and *H2-L*) — were also up-regulated in DENV1-infected mice (Table 2; Fig. 5), as were MHC class II molecules, like *H2-Ea*.

Real time PCR analyzes of modulated genes

We performed qPCR assays for 10 genes (*Stat1*, *Irf7*, *Irf1*, *Ifit3*, *Gbp4*, *Mx1*, *Oas1b*, *Ccl5*, *Psmb8* and *Tap1*) to confirm the gene expression data obtained from the microarrays. Primers used are listed in Table 1.

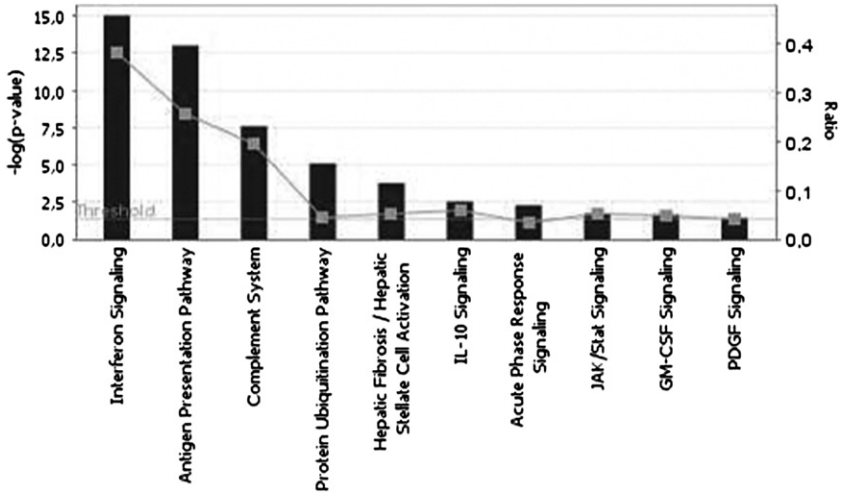

Fig. 4. Functional annotations associated with the 151 selected genes. The microarray data were analyzed using Ingenuity Pathways Analysis System. The *x*-axis displays selected biological functions and the *y*-axis the statistical significance (expressed as *p*-value, with a 0.05 threshold). The *p*-value measures how likely the observed association between a specific dataset would be if it was only due random chance. Ratio is calculated by taking the number of genes from dataset that participates in a Canonical Pathway, and dividing it by the total number of genes in that Canonical Pathway. JAK/Stat: Janus Kinase/Signal Transducer and Activator of Transcription; GM-CSF: Granulocyte and Macrophage Colony Stimulator Factor; PDGF: Platelet-derived Growth Factor.

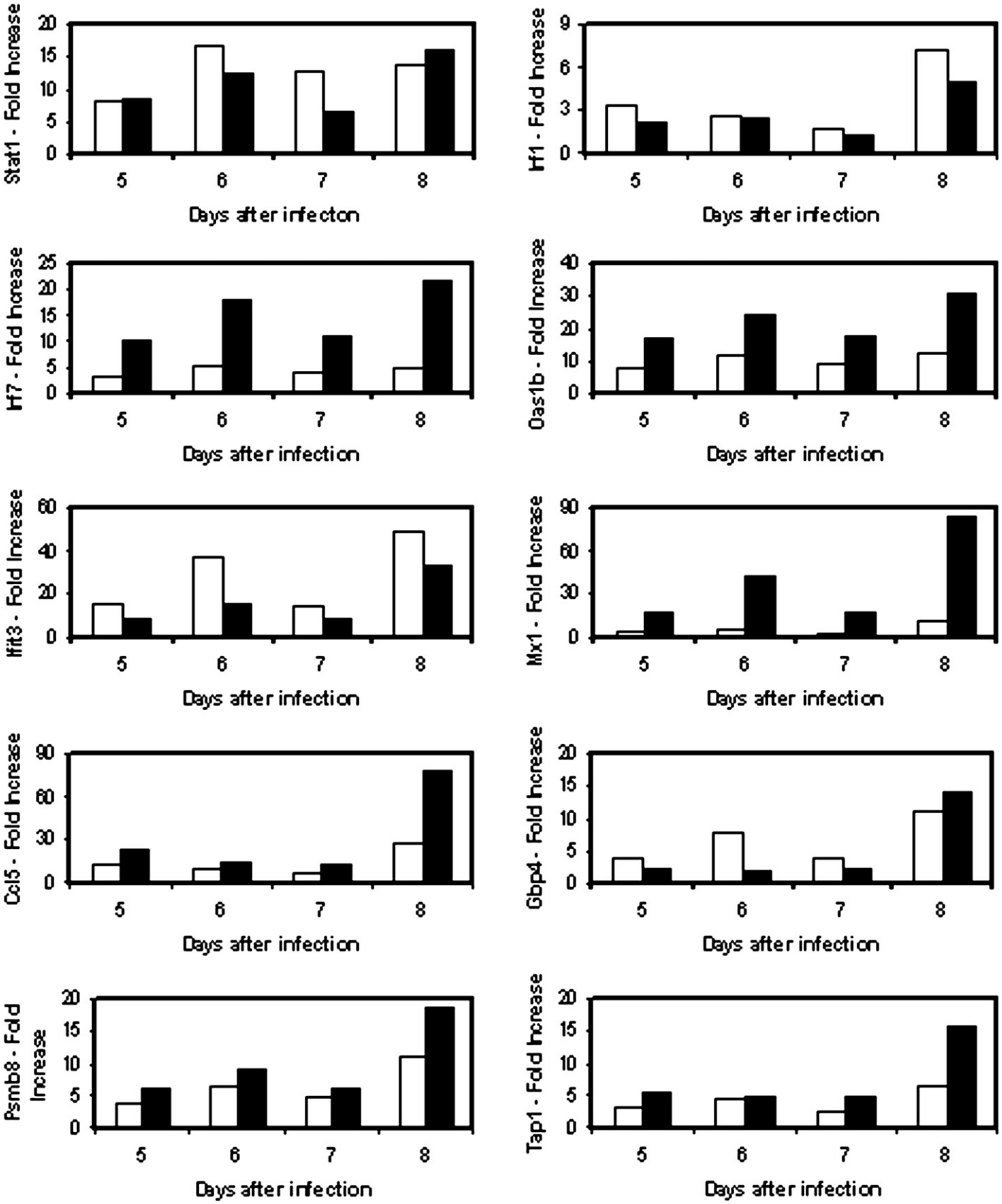

Fig. 5. Comparison of gene modulation levels measured by microarray analysis and qPCR. Comparison of levels of fold increase in gene expression of *Stat1*, *Irf1*, *Irf7*, *Ifit3*, *Gbp4*, *Mx1*, *Oas1b*, *Ccl5*, *Psmb8* and *Tap1*, measured by microarray (white bars) and qPCR (black bars).

The genes, *Stat1*, *Irf1* and *Irf7*, were selected because of their crucial role in IFN response after virus infection (Honda et al., 2005a,b). The IFN-stimulated genes, *Oas1b*, *Gbp4*, *Mx1*, *Ccl5*, *Ifit3*, *Tap1* and *Psmb8* that are genes involved in antiviral response and in antigen processing and presentation by MHC class I, were also included in qPCR analysis. mRNA levels detected by qPCR were consistent with microarray data for the

Table 1
Selected primers for qPCR, GenBank GeneID and expected molecular weight of amplicon

Gene	GenBank GeneID	Forward primer	Reverse primer	Amplicon
Stat1	20846	GAACGCGCTCTGCTCAA	TGCGAATAATATCTGGGAAAGTAA	190 bp
Irf7	54123	GCCAGGAGCAAGACCGTGTT	TGCCCCACCACTGCCTGTA	166 bp
Irf1	16362	TGTGTCGTCAGCAGCAGTCTCT	GTCTTCGGCTATCTTCCCTTCCT	153 bp
Ifit3	15959	CTGAAGGGGAGCGATTGATT	AACGGCACATGACCAAAGAGTAGA	182 bp
Oas1b	23961	TTCTACGCCAATCTCATCAGTG	GGTCCCCCAGCTTCTCCTTAC	172 bp
Mx1	17857	AACCCTGCTACCTTTCAA	AAGCATCGTTTTCTCTATTTC	183 bp
Gbp4[*]	17472	TGGGGGACACAGGCTCTACA	GCCTGCAGGATGGAACTCTCAA	144 bp
Ccl5	20304	GTGCCCACGTCAAGGAGTATTTCT	TGGCGGTTCCTTCGAGTGACAA	82 bp
Tap1	21354	GTGGCCGCAGTGGGACAAGAG	AGGGCACTGGTGGCATCATC	278 bp
Psmb8	16913	TGATGCTGCAGTACCGGGGGATGG	TAGCTCTGCGGCCAAGGTCGTAGG	222 bp
IFN-β	15977	CGCTGCGTTCCTGCTGTG	GATCTTGAAGTCCGCCCTGTAG	154 bp
IFN-α[**]	15964	GACTCATCTGCTGCTTGGAATGCAACCCTCC	GACTCACTCCTTCTCCTCACTCAGTCTTGCC	294 bp

[*] Annealing temperature 65 °C.
[**] Primer sequence described by Olson et al. (2001).

selected genes, although there were notable differences in the extent of gene induction measured by the array and qPCR methods (Fig. 5).

While a significant expression of IFN-stimulated genes was observed by microarray experiments, the up-regulation of IFN-α and -β transcripts was not detect. When qPCR analyzes of both genes were performed, the expression of IFN-β gene in DENV-infected mice was detected, compared to mock-infected animals, with a fold increase varying from 1.1 to 2.8, between days 5 and 8 post-infection (dpi). The IFN-α mRNA was not detected (data not shown).

Discussion

The clinical outcome of a viral infection is largely dependent on the balance between host response and viral replication rates. The ability of the virus to evade the host immune response is crucial to the development of disease in a susceptible host. Upon detection of viral infection, cells initiate a rapid antiviral response mediated by IFN and other cytokines that prevent the spread of the infection (Pasieka et al., 2006). Certain cellular proteins, including the toll-like receptors (TLRs) and other pattern-recognition receptors (PRRs), act as sensors and recognize dsRNA and other pathogen-associated molecular patterns (PAMPs), leading to IFN production which can then activate the IFN-response pathway, and creates an antiviral state in infected, as well as surrounding cells (Shaw and Palese, 2005). Shresta et al. (2004) demonstrated that IFN-α/β receptor-mediated action limits initial DENV replication in mouse extraneural sites and controls subsequent viral spread into the central nervous system.

We studied the gene transcription profile of mouse CNS infected with DENV1, to further contribute to the knowledge of dengue–vertebrate host interactions. The major pathways affected by DENV1 infection in the CNS of mice were those involved in IFN signaling, antigen presentation and processing, the complement cascade, and ubiquitination (Fig. 4). These changes are consistent with a robust innate immune response characterized in particular by genes induced by type I IFN (IFN-α/β). Our data are consistent with a previous study of peripheral blood mononuclear cells (PBMC) from rhesus monkeys, which demonstrated a profound up-regulation of ISGs following DENV1 infection (Sariol et al., 2007). Warke et al. (2008) have also recently demonstrated the expression of ISGs with known antiviral activity in human umbilical vein endothelial cells (HUVEC), monocytes and B cells that have been isolated from healthy volunteers and infected with DENV2. We observed a similar activation of the IFN-signaling pathway-induced gene expression following DENV1 infection of the CNS of mice (Table 2). The mechanisms involved in the antiviral activity remain unknown for most IFN-inducible proteins, one major role of these molecules is to reduce the activity of host enzymatic machinery, thus reducing viral replication, preventing infection of neighboring uninfected cells, and giving time for the host to arm an adaptive immune response.

Although the modulations in IFN-α/β genes were not detected in the microarrays experiments, the expression of IFN-β, but not IFN-α, could be quantified by qPCR. A possible explanation for the lack of modulation in IFN-α/β in the microarrays experiments could be due to the approach of using whole tissue instead cell culture systems. Changes in mRNA expression patterns in response to viruses that infected the nonrenewable cell populations of CNS may, however, be better studied in the intact host rather than in cell cultures (Venter et al., 2005). Other important point concerning IFN-α is the fact that it is modulated very early during viral infections, which could explain the negative result by qPCR. Moreover, low levels of IFN-α/β are capable to induce very strong ISGs stimulation as demonstrated in several microarray experiments (Bourne et al., 2007; Johnston et al., 2001; Sariol et al., 2007). Additionally, other authors had found the expression of ISGs in chimpanzee liver cells chronically infected with hepatitis C virus (Bigger et al., 2004) and in monkey PBMCs infected with DENV1 (Sariol et al., 2007), without detecting IFN-α/β transcripts.

In particular, one major ISG family up-regulated in the CNS of DENV1-infected mice encodes the 2′–5′ oligoadenylate system (2′–5′ OAS), which activates RNase L, inducing RNA degradation and reducing viral replication efficiency. It was shown that 2′–5′OAS genes confer resistance to infection with flaviviruses like hepatitis C virus (HCV) (Knapp et al., 2003), WNV (Kajaste-Rudnitski et al., 2006; Venter et al., 2005) and DENV (Warke et al., 2003). Resistance phenotype for flavivirus-induced disease in mice suggested that this phenotype was controlled by an autosomal dominant allele (*Flv*^{r}), that was identified as the 2′–5′OAS 1b (*Oas1b*). Susceptible mice show a premature stop codon, producing a protein lacking 30% of the C-terminal sequence as compared with the resistance counterpart (Perelygin et al., 2002). Scherbik et al. (2007) demonstrated that the knock-in of the *Oas1b*^{r} allele, which recovered the C-terminal region in susceptible mice, resulting in a resistant phenotype. Recently, Malathi et al. (2007) demonstrated that 2′–5′OAS activates RNase L, that produces small RNA cleavage products from self- or viral-RNA that induces the production of IFN-β through a pathway involving activation of retinoic acid-inducible gene-I (*RIG-I*), melanoma differentiation associated gene-5 (*MDA5*), and their interaction protein IPS1 (IFN-β promoter stimulator protein-1). The results demonstrated that OAS/RNase L has an effect on innate signaling pathways, enhancing IFN-β production, what could represent an interesting approach to the development of new antiviral therapies (Malathi et al., 2007).

Other antiviral ISG genes up-regulated in the CNS of mice following DENV1 infection include members of the Myxovirus protein family (Mx). In our hands, mouse CNS over-expressed *Mx1* (3.9–11.3 fold in microarray experiments and 5.8–36.5 in qPCR assays) and *Mx2* (6.9–20.0 fold in microarray experiments). It was recently shown that mice with deletion of the *Mx1* gene (*Mx1*−/−) are susceptible to infection with influenza virus H5N1 and 1918 pandemic influenza virus, whereas a high level of resistance was observed in *Mx1*(+/+) mice

Table 2
Selected genes up-regulated in brain tissue collected following DENV-1 infected mice

General Function	Specific Function	Biological Process	Gene Symbol	Entrez GeneID	Description	5 dpi	6 dpi	7 dpi	8 dpi
Immune response	Transcription	Interferon type I biosynthetic process	*Irf9*	16391	Interferon dependent positive acting transcription factor 3 gamma	3.52	5.59	4.6	4.68
			Irf7	54123	Interferon regulatory factor 7	3.01	5.24	3.9	4.99
			Irf8	15900	Interferon regulatory factor 8	2.21	1.88	3.05	8
		Cytokine and chemokine signalling	*Stat1*	20846	Signal transducer and activator of transcription 1	7.98	16.6	12.6	13.7
			Stat2	20847	Signal transducer and activator of transcription 2	1.62	4.78	2.68	5.36
			Nmi	64685	N-myc (and *Stat1*) interactor	2.78	3.47	2.4	3.8
		Positive regulator of interleukin-12	*Irf1*	16362	Interferon regulatory factor 1	3.23	2.55	1.79	7.12
		PML body	*Pml*	18854	Promyelocytic leukemia	1.97	2.3	2.23	2.13
			Sp100	20684	Nuclear antigen Sp100	3.03	3.38	1.72	2.86
	Endopeptidase	Antigen presentation	*Psmb8*	16913	Proteosome (prosome, macropain) subunit, beta type 8 (large multifunctional protease 7)	4.03	6.51	4.68	10.8
			Psmb9	16912	Proteosome (prosome, macropain) subunit, beta type 9 (large multifunctional protease 2)	3.96	6.56	2.43	14.3
	Transport	Antigen presentation	*Tap1*	21354	Transporter 1, ATP-binding cassette, subfamily B (MDR/TAP)	2.99	4.42	2.64	6.59
			Tap2	21355	Transporter 2, ATP-binding cassette, subfamily B (MDR/TAP)	3.59	2.75	2.84	13.1
	Antigen binding	Antigen presentation	*Lilrb4*	14728	Leukocyte immunoglobulin-like receptor, subfamily B, member 4	3.08	1.71	1.18	3.51
	MHC class II presentation	Antigen presentation	*H2-Ea*	14968	Histocompatibility 2, class II antigen E alpha	1.55	2.97	2.3	4.58
			H2-Ab1	14961	Histocompatibility 2, class II antigen A, beta 1	3.1	1.45	1.27	7.67
			Ctss	13040	Cathepsin S	2.64	2.81	2.98	6.78
			Cd74	16149	CD74 antigen (invariant polypeptide of major histocompatibility complex class II antigen-associated)	1.84	1.53	1.72	3.191
	MHC class I presentation	Antigen presentation	*H2-Q2*	15013	Histocompatibility 2, Q region locus 2	4.38	5.68	2.24	11.2
			H2-Q8	15019	Histocompatibility 2, Q region locus 8	3.4	3.88	2.47	5.53
			H2-Q7	15018	Histocompatibility 2, Q region locus 7	3.2	5.67	3.57	6.31
			H2-Q6	110557	Histocompatibility 2, Q region locus 6	2.81	5.25	3.43	7.32
			H2-Q5	15016	Histocompatibility 2, Q region locus 5	2.59	1.86	2.05	4.65
			H2-L	14980	Histocompatibility 2, D region	3.69	5.99	3.75	12.5
			H2-T9	15051	Histocompatibility 2, T region locus 9	3.86	2.34	2.43	5.07
			H2-T10	15024	Histocompatibility 2, T region locus 10	5.94	3.65	2.59	6.34
			H2-T22	15039	Histocompatibility 2, T region locus 22	3.74	2.34	2.12	5.09
			H2-T23	15040	Histocompatibility 2, T region locus 23	4.24	5.48	2.63	8.09
			H2-K1	14973	Histocompatibility 2, K1, K region	5.06	6.41	3.69	12.22
			B2m	12010	Beta-2 microglobulin	4.79	6.28	4.36	11.3
	GTP binding	Interferon-induced	*Gbp1*	14468	Guanylate nucleotide binding protein 1	4.41	1.46	1.59	9.57
			Gbp2	14469	Guanylate nucleotide binding protein 2	7.97	6.7	3.63	27.6
			Gbp4	17472	Guanylate nucleotide binding protein 4	3.82	6.81	3.48	12.99
			Gbp5	229898	Guanylate nucleotide binding protein 5	2.17	1.51	1.71	4.6
			Irgm	15944	Immunity-related GTPase family, M	8.86	11.5	7.48	12.4
			Gbp6	229900	Guanylate nucleotide binding protein 6	4.39	8.21	3.57	9.92
			BC057170	236573	cDNA sequence BC057170	3.56	2.49	3.09	7.44
			Mpa2l	100702	Macrophage activation 2 like	8.89	9.13	8.1	30.3
	RNA binding	Interferon-induced	*Oas1b*	23961	2′-5′oligoadenylate synthetase 1B	7.25	11.3	8.79	12.5
			Oas1g	23960	2′-5′oligoadenylate synthetase 1G	8.23	13.7	9.24	14.6
			Oasl1	231655	2′-5′oligoadenylate synthetase-like 1	3.84	7.16	2.86	9.03
			Oasl2	23962	2′-5′oligoadenylate synthetase-like 2	5.91	15.2	10.1	13.7
			Oas1a	246730	2′-5′oligoadenylate synthetase 1A	2.11	4.33	2.23	4.21
			Oas2	246728	2′-5′oligoadenylate synthetase 2	2.6	2.94	1.79	5.19
	DNA binding	Interferon-induced	*Sp110*	109032	Sp110 nuclear body protein	3.04	2.75	2.37	5.79
	Binding	Interferon-induced	*Ifit1*	15957	Interferon-induced protein with tetracopeptide repeats 1	8.82	23.7	12.4	37.6
			Ifit2	15958	Interferon-induced protein with tetracopeptide repeats 2	3.28	4.54	4.51	6.53
			Ifit3	15959	Interferon-induced protein with tetracopeptide repeats 3	15.4	37	14.8	49.2
	Helicase	Interferon-induced	*Ifih1*	71586	Interferon induce with helicase C domain 1	6.34	9.32	4.73	12.8
		Interferon type I biosynthetic process	*Dhx58*	230073	DEXH (Asp-Glu-X-His) box polypeptide 58	4.57	6.67	4.44	7.97
			Ddx58		DEAD (Asp-Glu-Ala-Asp) box polypeptide 58	4	6.35	4.27	6.43
	Protein binding	NC	*Ifi203*	15950	Interferon activated gene 203	2.47	2.85	2.56	7.44
		Interferon-induced	*Pyhin1*	236312	Pyrin and HIN domain family, member 1	6.45	1.48	1.93	11.25
		Apoptosis	*Bcl2a1a*	12044	B-cell leukemia/lymphoma 2 related protein A1a	2.32	1.87	2.2	3.91
	NC	NC	*Ifi205*	15952	Interferon activated gene 205	5.12	5.45	6.41	25.2
		Apoptosis	*Bcl2a1b*	12045	B-cell leukemia/lymphoma 2 realted protein A1b	3.09	1.97	1.89	3.15
			Bcl2a1c	12046	B-cell/leukemia/lymphoma 2 related protein A1c	3.28	1.41	1.75	7.93
	Receptor	Interferon-induced	*Ifitm1*	68713	Interferon-induced transmembrane protein 1	3.09	5.72	2.38	7.59
			Ifitm2	80876	Interferon-induced transmembrane protein 2	2.34	4.39	2.25	5.8
			Ifitm3	66141	Interferon-induced transmembrane protein 3	4.29	8.23	5.34	14.3

Table 2 *(continued)*

General Function	Specific Function	Biological Process	Gene Symbol	Entrez GeneID	Description	5 dpi	6 dpi	7 dpi	8 dpi
Immune response	Receptor	Cell adhesion	*Lgals9*	16859	Lectin, galactose binding, soluble 9	3.46	4.02	4.47	5.46
			Lgals3bp	19039	Lectin, galactosidase-binding, soluble, 3 binding protein	6.98	7.13	7.29	11.4
			Icam1	15894	Intercellular adhesion molecule 1	1.91	1.52	1.47	3.91
			Itgb2	16414	Integrin beta-2	1.74	1.51	1.74	3.06
			Siglec1	20612	Sialic acid binding Ig-like lectin 1, sialoadhesin	1.44	2.56	3.58	4.46
		B-cell activation	*Bst2*	69550	Bone marrow stromal cell antigen 2	7.58	14	8.75	16.8
		Cell proliferation	*Cd274*	60533	CD274 antigen	4.87	1.84	1.89	9.12
		Inhibition of proinflamatory cytokines	*Il10ra*	16154	Interleukin 10 receptor, alpha	1.93	2.79	1.71	3.68
		NC	*Ly6e*	17069	Lymphocyte antigen 6 complex, locus E	2.16	3.92	2.3	5.33
	GTPase	Interferon-induced	*Igtp*	16145	Interferon gamma induced GTPase	8.15	6.5	5.75	23.9
			Mx1	17857	Myxovirus (influenza virus) resistance 1	3.97	4.34	2.75	11.3
			Mx2	17858	Myxovirus (influenza virus) resistance 2	6.89	9.61	8.36	20
			Gvin1	74558	GTPase, very large interferon inducible 1	2.85	4.01	1.61	4
			Iigp2	54396	Interferon inducible GTPase 2	7.43	3.27	3.29	21
			Iigp1	60440	Interferon inducible GTPase 1	19.8	19.9	13.6	60.1
	Transcription	Interferon-induced	*Ifi204*	15951	Interferon activated gene 204	5.5	4.06	6.05	19.7
	Exonulcease	Interferon-induced	*Isg20*	57444	Interferon-stimulated protein	1.38	2.31	1.82	4.2
	Kinase	Interferon-induced	*Eif2ak2*	19106	Eukaryotic translation initiation factor 2-alpha kinase 2	3.9	7.07	4.36	7.84
	Cytokine/chemokine	Chemotaxis	*Ccl5*	20304	Chemokine (C-C motif) ligand 5	13.1	9.37	7.33	26.9
			Ccl12	20293	Chemokine (C-C motif) ligand 12	3.97	9.89	6.14	23
			Cxcl10	15945	Chemokine (C-X-C motif) ligand 10	2.37	2.47	2.84	20.5
		Apoptosis	*Tnfsf10*	22035	Tumor necrosis factor (ligand) superfamily, member 10	1.47	2.8	1.86	2.91
	Peptidase	Complement activation	*Cfb*	14962	Histocompatibility 2, complement component factor B	7.52	5.71	6.61	19.7
			C2	12263	Complement component 2 (within H2-S)	2.2	2.42	1.9	5.89
			C1r	50909	Complement component 1, r subcomponent	4.52	1.73	2.39	5.62
	Peptidase inhibitor	Complement activation	*C4b*	12268	Complement component 4B (Childo blood group)	2.69	2.41	2.4	5.08
	Endopeptidase inhibitor	Apoptosis	*Serpina3g*	20715	Serine (or cysteine) proteinase inhibitor, clade A, member 3G	5.29	1.52	2.83	7.88
	NC	Complement activation	*C1qb*	12260	Complement component 1, q subcomponent, beta polypeptide	1.41	1.91	1.91	3.26
		Apoptosis	*Bcl2a1d*	12047	B-cell leukemia/lymphoma 2 related protein A1d	2.4	1.58	1.53	3.39
	Caspase activity	Apoptosis	*Casp1*	12362	Caspase 1	2.88	2.01	2.04	4.84
	Poly-A-polymerase	NC	*Parp9*	80285	Poly (ADP-ribose) polymerase family, member 9	4.53	6.1	3.32	9.47
		Virus response	*Zc3hav1*	78781	Zinc finger CCCH type, antiviral 1	4.25	3.92	2.38	6.85
	Apoptosis	IFN-induced	*Sp110*	109032	Sp110 nuclear body protein	1.31	3.95	2.07	4.92
	Catalytic activity	Virus response	*Rsad2*	58185	Radical *S*-adenosyl methionine domain containing 2	2.64	2.48	2.03	7.77
		IFN-induced	*Samhd1*	56045	SAM domain and HD domain 1	1.78	2.01	1.89	5.65
	dTTP biosynthesis	LPS response	*Tyki*	22169	Thymidylate kinase family LPS-inducible member	1.2	2.51	1.76	3.73
	NC	IFN-induced	*Ifi44*	99899	Interferon-induced protein 44	7.55	12.8	5.51	16.1
			Ifi27	76933	Interferon, alpha-inducible protein 27	8.62	6.24	12.9	21
	NC	Interferon-induced	*Ifi47*	15953	Interferon gamma inducible protein 47	9.47	12.4	8.7	38
	NC	NC	*Ifi202b*	26388	Interferon activated 202B	8.29	11.5	8.38	40.1
			Plac8	231507	Placenta-specific 8	15.2	14.1	12.4	33
Defense response	GPI anchored	Cell proliferation	*Ly6a*	110454	Lymphocyte antigen 6 complex, locus A	3.11	2.40	2.38	10.79
		NC	*Ly6c1*	56778	Lymphocyte antigen 6 complex, locus C	1.82	2.14	1.62	5.3
			Ly6f	17071	Lymphocyte antigen 6 complex, locus F	3.33	1.67	2.7	7.41
	Protein binding	Cell adhesion	*Ly9*	17085	Lymphocyte antigen 9	2.53	1.69	1.81	3.39
	Macrophage associated	NC	*Mpeg1*	17476	Macrophage expressed gene 1	1.51	2.91	2.3	4.41
Ubiquitin cycle	Ubiquitin ligase	Interferon-induced	*Dtx31*	209200	Deltex 3-like (*Drosophila*)	3.04	3.73	3.59	4.74
			Herc5	67138	Hect domain and RLD5	3.48	4.15	3	6.98
			Trim25	217069	Tripartite motif protein 25	3.23	4.52	3.57	4.61
		Protein modification	*Ube2l6*	56791	Ubiquitin-conjugating enzyme E2L6	1.33	2.08	3.28	2.59
			Trim21	20821	Tripartite motif protein 21	3.52	6.72	3.3	9.68
	Ubiquitin activating	Protein modification	*Ube1l*	74153	Ubiqutin-activating enzyme E1-like	1.84	4.32	2.9	5.91
	Protein binding	Interferon-induced	*Isg15*	53606	ISG15 ubiquitin-like modifier	10.4	22.3	9.41	26.9
	Peptidase	Interferon-induced	*Usp18*	24110	Ubiquitin specific protease	18	31.6	18.3	26.9
Signal transduction	Receptor	Apoptosis	*Tspo*	12257	Translocator protein	1.51	2.06	1.82	2.68
		NC	*Fgl2*	14190	Fibrinogen-like protein 2	1.94	1.42	1.67	3.43
			Ms4a6d	68774	Membrane-spaning 4-domains, subfamily A, member 4D	4.92	3.2	2.16	5.11
			Ms4a4c	64380	Membrane-spaning 4-domains, subfamily A, member 4C	4.2	2.85	-1.03	14.48
			Ms4a6b	293749	membrane-spanning 4-domains, subfamily A, member 6B	3.05	1.52.	2.18	3.51
Chaperone	ATP binding	Protein folding	*Tor3a*	30935	Torsin family 3, member A	2.66	6.12	4.53	19.1
Metabolism	Phospholipase	Lipid catabolism	*Pld4*	104759	Phospholipase D family, member 4	2	2.16	1.48	3.71
Inflamatory response	Oxireductase activity	Phagocytic killing	*Cybb*	13058	Cytochrome b-245, beta polypeptide	2.96	1.77	1.18	8.21
	Receptor		*Cd14*	12475	CD14 antigen	3.27	1.68	1.76	2.01

(*continued on next page*)

Table 2 *(continued)*

General Function	Specific Function	Biological Process	Gene Symbol	Entrez GeneID	Description	5 dpi	6 dpi	7 dpi	8 dpi
NC	Poly-A-polymerase	Transcription regulation	*Parp14*	547253	Poly (ADP-ribose) polymerase family, member 14	5.42	6.51	2.71	13.2
		NC	*Parp12*	243771	Poly (ADP-ribose) polymerase family, member 12	4.12	4.51	4.31	7.9
	Helicase	NC	*BC013672*	234311	cDNA sequence BC013672	5.65	4.51	2.33	7.62
			BC013672	234311	cDNA sequence BC013672	8.96	11.4	3.86	19.8
	Protein transport	NC	*4930599N23Rik*	75379	RIKEN cDNA 4930599N23 gene	2.11	2.95	1.74	2.07
			Mitd1	69028	RMIT, microtubule interacting and transport, domain containing 1	1.8	1.66	1.55	3.17
	Kinase	NC	*Mlkl*	74568	Mixed lineage kinase domain-like	4.29	4.48	2.3	3.96
	DNA binding	NC	*Zbp1*	58203	Z-DNA binding protein 1	2.79	2.48	1.96	4.98
		Apoptosis	*Scotin*	66940	Scotin	3.49	2.59	3.77	2.69
	Receptor	Interferon-induced	*Rtp4*	67775	Receptor transporter protein 4	2.75	4.1	2.4	2.64
	Protein/nucleic acid binding	Interferon-induced	*Trim34*	94094	Tripartite motif protein 34	2.47	2.72	2.04	2.72
		NC	*Trim30*	20128	Tripartite motif protein 30	3.93	5.54	2.82	8.05
	NC	Cell proliferation	*Slfn2*	20556	Schlafen 2	3.32	2.51	2.02	5.3
NC	NC	NC	*BC006779*	229003	cDNA sequence BC006779	2.24	3.67	2.34	3.88
			Epsti1	108670	Epithelial stromal interaction 1 (breast)	2.24	4.41	2.89	4.64
			D12Ertd647e	52668	DNA segment, Chr 12, ERATO Doi 647, expressed	2.96	3.06	2.24	1.86
			Samd9l	209086	Sterile alpha motif domain containing 9-like	4.04	6.67	4.16	13
			D14Ertd668e	219132	DNA segment, Chr 14, ERATO Doi 668, expressed	3.56	5.97	3.3	10.4
			Rnf213	629974	Ring finger protein 213	4.19	8.44	3.43	7.04
			Phf11	219131	PHD finger protein 11	9.3	8.5	4.53	22.8
			0610037M15Rik	68395	RIKEN cDNA 0610037M15 gene	3.59	6.29	3.07	6.14
			9830115L13Rik	319257	RIKEN cDNA 9830115L13 gene	3.14	5.85	8.29	5.27
			A630077B13Rik	215900	RIKEN cDNA A630077B13 gene	2.85	1.36	1.32	7.16
			C4a	625018	Complement component 4A (Rodgers blood group)	1.73	2.94	2.62	5.25
			Gp49a	14727	Glycoprotein 49A	3.95	1.26	1.61	4.59
			Drld	114573	Differentially regulated in lymphoid organs and differentiation	1.87	1.33	1.88	3.54
			H2-T17	15032	Histocompatibility 2, T region locus 17	5.46	3.17	1.37	9.83
			Rnf213	629974	Ring finger protein 213	4.2	8.44	3.43	7.05

* Not classified.
1. Genes with more than one probe had their intensity averaged.
2. Gene functional classification was done using NCBI Entrez Gene (www.ncbi.nih.gov) and Gene Ontology (www.geneontology.org) database.

(Tumpey et al., 2007). *Mx1, Mx2* and *MxA* are up-regulated in HUVEC cells infected with DENV2 (Warke et al., 2003). PBMCs from monkeys infected with dengue virus type-1 also exhibit up-regulation of *Mx1* and *Mx2* (Sariol et al., 2007), giving support to our findings, however, the potential role of these family gene in dengue virus infection needs to be better evaluated. Recently, Simmons et al. (2007) demonstrated that the levels of transcription of 24 genes, including *Mx1* and *Mx2*, were attenuated in patients with DSS when comparing with patients with DHF, suggesting an important role of these genes in the severity of dengue infection.

In this study, genes involved in antigen processing (*Psmb8* and *Psmb9*, or *LMP7* and *LMP2*), in transportation of antigens to endoplasmic reticulum (*Tap1* and *Tap2*), and in the presentation of major histocompatibility complex (MHC) class I and II at the cell surface were up-regulated. MHC-encoded IFN-γ-inducible low molecular weight proteins (LMP2, 7 and 10) form the immunoproteasome. This degradative system seems to have different substrate specificity than that of a proteasome (Van de Eynde and Morel, 2001; Groettrup et al., 1996). The immunoproteasome was observed in neuronal cells in some neurodegenerative disorders like Huntington's Disease (Diaz-Hernandez et al., 2003), Amylotropic Lateral Sclerosis (Cheroni et al., 2005) and Alzheimer's Disease (Mishto et al., 2006). MHC class I levels are low in the intact CNS and is confined to blood vessels (Gehrmann et al., 1991, 1993; Vass and Lassmann, 1990). MHC class II is consistently found on meningeal macrophages, choroid plexus macrophages and perivascular cells (Gehrmann et al., 1991, 1993, 1995; Graeber et al., 1989, 1992; Hickey and Kimura, 1988; Hickey et al., 1992; Vass and Lassmann, 1990). Additionally, MHC class II seems to be constitutively expressed on a subpopulation of resident microglia (Streit et al., 1989).

Three main hypotheses could be raised to explain the expression of antigen processing and presentation in mice CNS after dengue virus infection: expression by neuron infected cells; expression by accessory cells, like microglia, oligodendrocytes and endothelial cells; and expression by infiltrated cells, like B cells or monocytes/macrophages from periphery. Classically, neurons do not participate in antigen processing and presentation, and are generally incapable of expressing MHC molecules in their surface (Gogate et al., 1996; Joly and Oldstone, 1992). However, it was recently demonstrated that during acute infection with mouse hepatitis virus (MHV), MHC class I is expressed *in vivo* by neurons, oligodendrocytes, microglia and endothelia, and MHC class II is expressed only by microglia. These data indicates that neurons cells have the potential to present antigen to T cells and thus be damaged by direct antigen-specific interactions with $CD8^+$ T lymphocytes (Redwine et al., 2001). Recently, was demonstrated the expression of LMP genes in murine neuronal cells after IFN-γ treatment (Yang et al., 2006). In contrast, inflammatory cytokines (IFN-γ and TNF-α) can induce the expression of MHC class II molecules on the cell surface of astrocytes (Vass and Lassmann, 1990), suggesting that cytokines produced by infected cells could trigger the gene expression in surrounding cells. Finally, we previously demonstrated that DENV1 FGA/89-infected animals present mild chronic lymphoystiocitic leptomeningitis (Bordignon et al., 2007); thus, the up-regulation of genes involved in antigen processing and presentation that we detected in our studies could be a result of cell infiltration in the CNS (such as monocytes/macrophages and lymphocytes).

We observed the up-regulation of ISGs (*Isg*15, *Ube1l*, *Ube2l6* and *Usp18*) involved in the ubiquitin-like process, known as protein ISGylation. *Isg15* has an amino-acid sequence with considerable homology to that of ubiquitin, and is conjugated and deconjuganted to target proteins through a set of reactions that involve activating (*Ube1l*; Yuan and Krug, 2001), conjugating (*Ube2l6*; Kim et al., 2004) and deconjugating enzymes (*Usp18* or *Ubp43*) (Malakhov et al., 2002). Protein ISGylation has been implicated in fetal development and innate immunity (Rempel et al., 2007; Ritchie et al., 2006). A recent study demonstrated that mice deficient in *Usp18* (deconjugating enzyme) are resistance to fatal lymphocytic choriomeningitis virus

(LCMV) and vesicular stomatitis virus (VSV) infections. *Usp18* knockout mice have an enhanced interferon-mediated response, which may underlie the low viral RNA replication efficiency and antigen expression in the brains of infected animals (Ritchie et al., 2006). Malakhova et al. (2006) demonstrated that *Ubp43* (*Usp18*) binds to the IFNAR2 receptor subunit, blocking the receptor's interaction with JAK1, and thus inhibiting JAK1 activity (Malakhova et al., 2006). The authors showed that Usp18 functions as a negative regulator of the IFN-mediated response, which is essential for ensuring an appropriate and controlled cellular response to type I IFN. Conversely, inhibition of *Usp18* enhances the IFN response, presenting a potential alternative target for antiviral therapies. The role of protein ISGylation in the antiviral response has recently been demonstrated for influenza B virus (Yuan and Krug, 2001), LCMV, VSV (Ritchie et al., 2006), and Sindbis virus (Lenschow et al., 2005). The expression of genes involved in this pathway is modulated by viral infection mediated by the *Flaviviridae* family, including hepatitis C and DENV1 infection in chimpanzees and monkeys, respectively, and WNV infection in mice (Bigger et al., 2004; Sariol et al., 2007; Venter et al., 2005). Recently, Warke et al. (2008) shows up-regulation of *USP18* gene in HUVEC cells, and in human monocytes and B cells infected with DENV2. Overall, these findings suggest that a common pathway is modulated by IFN in response to virus infection in vertebrate hosts. However, the role of this pathway in human DENV infections needs to be confirmed in future studies.

Our findings demonstrate the up-regulation of genes involved in the complement system, H2-Bf (Complement factor B), C1qb, C1r, C2 and C4 — with mRNA levels increasing 1.4- to 5.8-fold between dpi 5 and dpi 8 — in Swiss mice infected with DENV1 FGA/89 (Table 2; Fig. 4). The complement system is a family of more than 30 proteins, including cell surface receptors, which recognize pathogen-associated molecular patterns (PAMPs), altered self-ligands, or immune complexes (Carroll, 2004). Complement activation was proposed 30 years ago as a major event in the development of DHF/DSS (Bokisch et al., 1973). Complement can be activated by non-structural protein NS1 (soluble or cell-associated), and enhanced by anti-NS1 antibodies, leading to local or systemic generation of anaphylatoxins and terminal complex SC5b-9. Plasma levels of NS1 and terminal complex SC5b-9, from 163 patients, correlate with disease severity (Avirutnan et al., 2006). Similarly, activation of the complement system in dengue virus infection could contribute to the pathogenesis of vascular leakage in DHF/DSS (Avirutnan et al., 2006). Mehlhop and Diamond (2006) also demonstrated an important role for complement activation in protection and in priming the adaptive immune response to WNV infections. They showed that mice deficient in C1q, C4, factor B or D, and infected with WNV, had an increased mortality rate, suggesting that the different activation pathways (classical, lectin and alternative) act together to limit WNV infection spreading. A deficiency in the alternative pathway led to a delay in splenic clearance and a blunted T-cell response. Deficiencies in the classical and lectin pathways were associated with decreased splenic infection and deficits in the B- and T-cell responses to WNV infection in the murine model.

We previously demonstrated that animals infected with DENV1 FGA/89 develop mild chronic lymphoystiocitic leptomeningitis without encephalitis, with complete viral clearance at 30 dpi (Bordignon et al., 2007). We demonstrated that animals developed a strong innate immune response, and exhibited an up-regulation of antiviral ISGs that seems to be responsible in the control of dengue infection in mice CNS, preventing the death of the animals. Our findings of changes in gene expression during DENV1 infection in the mouse CNS are consistent with recent results obtained by Sariol et al. (2007) in PBMCs from monkeys infected with DENV1, and by Warke et al. (2008) in human monocytes, B cells and HUVEC cells infected with DENV2. A better understanding of innate immunity mechanism acting against viral infections offers the possibility of new potential strategies for developing therapies against dengue infection. Indeed, the potential modulation of innate immunity to improve the antiviral response in an infected host, limiting viral replication and reducing the severity of disease, may be an effective strategy to fight DENV infection.

Material and methods

Viruses and infection of animals

Virus stocks were amplified in C6/36 cells and purified in a sucrose gradient as described by Gould and Clegg (1985). Mock was prepared from non-infected C6/36 cell supernatants at the same time points and processed following the same protocols. Virus titer was determined by the focus-forming unit technique in C6/36 cells (ffu_{C636}), described by Dèspres et al. (1993). The FGA/89 viral strain was kindly supplied by Dr. Philippe Desprès, from the *Unité des Interactions Moléculares Flavivirus-Hôtes* at the Pasteur Institute, Paris, France. FGA/89 was isolated in South America in 1989 from a patient with DF. Dèspres et al. (1998) had shown that this is an avirulent strain for mice, however, recently we demonstrated that although mice survive without signals of encephalitis, this strain causes leptomeningitis in infected mice (Bordignon et al., 2007).

To avoid bias in the experiments, animals used in the study were grouped together after birth (from different females), assorted and separated into two groups of 30 newborn animals. Forty eight hours after birth, Swiss mice underwent intracerebral (IC) inoculation with 8000 ffu_{C636} of DENV1 FGA/89 or were mock-infected. At days five, six, seven and eight post-infection (dpi), five animals from both the mock-infected and FGA/89-infected groups were killed, and their encephalus was retrieved and pooled for biological and gene expression analyses. Animal experiments were approved by the ethical committee on animal experimentation of the Oswaldo Cruz Foundation (CEP/FIOCRUZ 264/05) and the Federal University of Paraná (CEP/UFPR 23075.002348/2007-14).

Viral load in the CNS of infected mice

We extracted RNA from pooled brain tissues of mock and DENV1-infected animals using RNeasy Mini Kit (Qiagen) following manufactures instructions. Viral RNA load was determined by quantitative RT-PCR (qRT-PCR), as described by Poersch et al. (2005). The qRT-PCR curves were normalized using murine glyceraldeyde-3-phosphate dehydrogenase (*Gapdh*), as described previously (Bordignon et al., 2007).

RNA samples and microarrays hybridization

RNA obtained from the brains of infected and mock-infected animals was amplified *in vitro* using the Amino Allyl MessageAmp™ aRNA Amplification kit (Ambion Inc., Austin, TX, USA) according to manufacturer's instructions. The quantity and quality of the amplified RNA (aRNA) were evaluated by spectrophotometry at 260/280 nm. Before hybridization experiments, microarrays were re-hydrated with 3× SSC/0.2% sodium dodecyl sulfate (SDS) and cross-linked with 65 mJ under UV irradiation. Microarrays were washed with distilled water and 95% ethanol, and then blocked with anhydride succinic solution. This pretreatment blocks amines from binding the microarrays prior to hybridization, reducing the background and providing a better distribution of DNA across the surface of the spot. The murine microarray — produced in the Virginia Commonwealth University (USA) — contains 38,467 mouse exonic evidence-based oligonucleotide (MEEBO) 70-mer probes, targeting 35,302 mouse genes and 3482 controls.

For microarray experiments, aRNA (3 μg) was reverse transcribed with 2 nmol of random hexamers (Invitrogen), 25 nmol of each dNTP, 2 μl of reverse transcriptase (ImProm-II™ Reverse Transcriptase/Promega) and 60 U of RNAse OUT™ (Invitrogen) at 42 °C for 2 h. RNA was denatured with 0.03 N NaOH at 70 °C for 10 min and the pH of solution was neutralized with 0.03 N HCl. After a wash step with water using Microcon 30, the volume was adjusted to 22 μl and the material was used to synthesize a second-strand DNA at 37 °C for 2 h using

20 µl of Random Primers Solution (1×) and 0.8 U of Klenow polymerase (BioPrime DNA Labeling System Kit), 6 nmol of dATPs, dGTPs and dTTPs, 3 nmol of dCTPs and 2 nmol of dCTP-Cy3 or dCTP-Cy5. Finally, the samples were washed twice with DEPC water using Microcon 30 filters (Amicon) and diluted in hybridization solution (5× SSC, 4.2× Denhardt's solution, 0.21 mg/ml ssDNA, 0.42% SDS and 42% formamide) to a final volume of 120 µl. They were then heat-denatured and loaded using a workstation GeneTAC HybStation (PerkinElmer) for hybridization at 42 °C for 16 h. The arrays were washed twice for 5 min with a solution containing 0.01% SDS and 0.5× SSC, and a further two times with 0.06×SSC solution. Finally, fluorescence was measured in a scanner (Array Express, PerkinElmer) at 550 nm and 649 nm for Cy3 and Cy5, respectively.

Data analysis

Microarray images were analyzed with the Spot software (Beare and Buckley, 2004). Background extraction and data normalization were performed by the limma software (Smith, 2004). Single channel intensity from all technical replicates (hybridizations) for each day of mock and FGA/89 samples were averaged and differential expression was assessed by means of a two class unpaired SAM test (Tusher et al., 2001), using two-fold change and 1% FDR (false discovery rate) as thresholds. Aiming to increase the stringency of the differential expression attribution, samples collected on the different days were considered as biological replication unity. As a consequence, we loose the ability to select point-specific differences, but increase the power to confidently select genes that were changed in a more general trend, what is more related to the approach used, namely a whole tissue and late days analysis.

Selected genes from the microarray data were also analyzed using the Ingenuity Pathways Analysis software (IPA; Ingenuity Systems®, www.ingenuity.com; Redwood City, CA, USA). Ingenuity Pathways Analysis Knowledge Base is a curate database, constructed based on scientific evidence obtained from hundreds of thousands of journal articles, textbooks, and other data sources. A list of all genes modulated obtained by microarray experiments were analyzed by IPA software, to define which well-characterized cell signaling and metabolic pathways are most relevant during DENV infection in mice CNS. The significance (*p*-values) of the association between the dataset and the canonical pathway was measured by comparing the number of user-specified genes of interest participating in a given pathway, relative to the total number of occurrence of these genes in all pathway annotations, stored in Ingenuity Pathways Knowledge Base. Fisher's exact test was used to calculate a *p*-value determining the probability that the association between the genes in the dataset and the canonical pathway is explained by chance only.

Relative quantification of mRNA levels by quantitative PCR (qPCR)

Messenger RNA (mRNA) levels from 10 genes (*Stat1, Irf7, Irf1, Ifit3, Gbp4, Mx1, Oas1b, Ccl5, Psmb8* and *Tap1*) were determined by qPCR. RNA samples isolated from dengue- and mock-infected mice brain tissues were reverse transcribed using ImProm-II™ (Promega, Madison, WI) and oligo-dT primers (20 µM) following the manufacturer's protocol. The resulting cDNAs were amplified by PCR with SYBR Green master mix (Applied Biosystems, Inc.) in an ABI PRISM 7000 Sequence Detection System (Applied Biosystems, Inc.) The following cycle was used for amplification: 50 °C for 2 min, 96 °C for 10 min, followed by 40 cycles of 96 °C for 15 s, 60 °C for 30 s, and 72 °C for 1 min (primers sequences are showed in Table 1). Melting curves were used to verify product specificity. The murine housekeeping gene encoding *Gapdh* was also included, for normalization of mRNA levels as described previously (Bordignon et al., 2007). Levels of mRNA for each selected gene were recorded as fold increase induced by dengue virus infection in the CNS of mice. Fold increase was the amount of mRNA for each gene from DENV1-infected animal tissues divided by amount of mRNA from mock-infected animal tissues taken at the same time points.

Immunohistochemistry

Mice from DENV1 FGA/89-infected and mock-infected groups were killed at 10 dpi; brain tissues were collected and fixed in 10% buffered formalin. Fixed tissues were paraffin embedded, sectioned, and stained with a flavivirus group-specific monoclonal antibody 4G2 (1:100). Goat anti-rat immunoglobulin conjugated to peroxidase-labeled dextran polymer (Envision$^+$/Peroxidase, DakoCytomation®) was used as secondary antibody, and liquid DAB (DakoCytomation®) was used for visualization. Antigen recovery was performed using the ImmunoRetriver Bio SB® Kit.

Acknowledgments

We are indebted with Dr. Peter W. Mason, from Texas University Medical Branch, Galveston, Texas, USA (UTMB) for his critical reading of the manuscript. We also thank Ana Paula Camargo Martins for technical assistance. The authors thank CNPq, Fundaçã o Araucá ria, Fundo Paraná and Fiocruz for financial support.

References

Avirutnan, P., Punydee, N., Noisakran, S., Komoltri, C., Thiemmeca, S., Auethavornanan, K., Jairungsri, A., Kanlaya, R., Tangthawornchaikul, N., Puttikhunt, C., 2006. Vascular leakage in severe dengue virus infections: a potential role for nonstructural viral protein NS1 and complement. J. Infect. Dis. 193, 1078–1088.

Beare, R. & Buckley, M., 2004. Spot: cDNA microarray image analysis users guide. http://spot.cmis.csiro.au/spot/doc/Spot.pdf.

Blatch, G.L., Lassle, M., 1999. The tetratricopeptide repeat: a structural motif mediating protein–protein interactions. Bioessays 21, 932–939.

Bigger, C.B., Guerra, B., Brasky, K.M., Hubbard, G., Beard, M.R., Luxon, B.A., Lemon, S.M., Lanford, R.E., 2004. Intrahepatic gene expression during chronic hepatitis C virus infection in chimpanzees. J. Virol. 78 (24), 13779–13792.

Bordignon, J., Strottman, D.M., Mosimann, A.L.P., Probst, C.M., Stella, V., Noronha, L., Zanata, S.M., Duarte dos Santos, C.N., 2007. Dengue neurovirulence in mice: identification of molecular signatures in E and NS3 helicase domains. J. Med. Virol. 79 (10), 1506–1517.

Bokisch, V.A., Top Jr., F.H., Russell, P.K., Dixon, F.J., Muller-Eberhard, H.J., 1973. The potential pathogenic role of complement in dengue hemorrhagic shock syndrome. N. Engl. J. Med. 289, 996–1000.

Bourne, N., Scholle, F., Silva, M.C., Rossi, S.L., Dewsburry, N., Judy, B., De Aguiar, J.B., Leon, M.A., Estes, D.M., Fayzulin, R., Mason, P.W., 2007. Early production of type I interferon during West Nile virus infection: role for lymphoid tissues in IRF3-independent interferon production. J. Virol. 81 (17), 9100–9108.

Carroll, M.C., 2004. The complement system in regulation of adaptative immunity. Nat. Immunol. 5, 981–986.

Cheroni, C., Peviani, M., Cascio, P., Debiasi, S., Monti, C., Bendotti, C., 2005. Accumulation of human SOD1 and ubiquitinated deposits in the spinal cord of SOD1G93A mice during motor neuron disease progression correlates with a decrease of proteasome. Neurobiol. Dis. 18, 509–522.

Clyde, K., Kyle, J.L., Harris, E., 2006. Recent advances in deciphering viral and host determinants of dengue virus replication and pathogenesis. J. Virol. 80 (23), 11418–11431.

D'Andrea, L.D., Regan, L., 2003. TPR proteins: the versatile helix. Trends Biochem. Sci. 28, 655–662.

Delhaye, S., Paul, S., Blakqori, G., Minet, M., Weber, F., Staeheli, P., Michiels, T., 2006. Neurons produce type I interferon during viral encephalitis. Proc. Natl. Acad. Sci. U. S. A. 103 (20), 7835–7840.

Dèspres, P., Frenkiel, M.P., Deubel, V., 1993. Differences between cell membrane fusion activites of two dengue type-1 isolates reflect modifications of viral structure. Virology 196, 209–219.

Dèspres, P., Frenkiel, M.P., Ceccaldi, P.E., Duarte dos Santos, C.N., Deubel, V., 1998. Apoptosis in the mouse central nervous system in response to infection with mouse-neurovirulent dengue viruses. J. Virol. 72, 823–829.

Diaz-Hernandez, M., Hernandez, F., Martin-Aparicio, E., Gómez-Ramos, P., Moran, M.A., Casiano, J.G., Ferrer, I., Avila, J., Lucas, J.J., 2003. Neuronal induction of the immunoproteasome in Huntington's disease. J. Neurosci. 23, 11653–11661.

Fearon, D.T., 1999. Innate immunity and the biological relevance of the acquired immune response. Q. J. Med. 92, 235–237.

Gehrmann, J., Monoco, S., Kreutzberg, G.W., 1991. Spinal cord microglial cells and DRG satellite cells rapidly respond to transaction of the rat sciatic nerve. Restor. Neurol. Neurosci. 2 (181), 198.

Gehrmann, J., Gold, R., Linington, C., Lannes-Vieira, J., Wekerle, H., Kreutzberg, G.W., 1993. Microglial involvement in autoimmune inflammation of the central and peripheral nervous system. Glia 7, 50–59.

Gehrmann, J., Matsumoto, Y., Kreutzberg, G.W., 1995. Microglia: intrinsic immuneffector cell of the brain. Brain Res. Brain Res. Rev. 20, 269–287.
Gogate, N., Swoveland, P., Yamabe, T., Verma, L., Woyciechowska, J., Tarnowska-Dzidusko, E., Dymecki, J., Dhib-Jalbut, S., 1996. Major histocompatibility comple class I expression on neurons in subacute sclerosing panencephalitis and experimental subacute measles encephalitis. J. Neuropathol. Exp. Neurol. 55, 435–443.
Gould, E.A., Clegg, J.C.S., 1985. Growth, titration and purification of togaviruses. In: Mahy, B.W.J. (Ed.), Virology: A pratical approach. IRL Press, Washington, DC, pp. 43–78.
Graeber, M.B., Streit, W.J., Kreutzberg, G.W., 1989. Identity of ED2-positive perivascular cells in rat brain. J. Neurosci. Res. 22, 103–106.
Graeber, M.B., Streit, W.J., Bueringer, D., Sparks, D.L., Kreutzberg, G.W., 1992. Ultrastructural location of major histocompatibility complex (MHC) class II positive perivascular cells in histologically normal human brain. J. Neuropathol. Exp. Neurol. 51, 303–311.
Groettrup, M., Kraft, R., Kostka, S., Standera, S., Stohwasser, R., Kloetzel, P.M., 1996. A third interferon-gamma induced subunit exchange in the 20S proteasome. Eur. J. Immunol. 26, 863–869.
Gubler, D.J., 1997. Dengue and dengue hemorrhagic fever: its history and resurgence as a global public health problem. In: Gubler, D.J., Kuno, G. (Eds.), Dengue and Dengue Hemorrhagic Fever. CABI Publishing, New York, NY, pp. 1–22.
Halstead, S.B., 1988. Pathogenesis of dengue: challenges to molecular biology. Science 239 (4839), 476–481.
Halstead, S.B., O'Rourke, E.J., 1977. Dengue viruses and mononuclear phagocytes. I. Infection enhancement by non-neutralizing antibody. J. Exp. Med. 146 (1), 201–217.
Hickey, W.F., Kimura, H., 1988. Perivascular microglia are bone marrow derived and present antigen in vivo. Science 239, 290–292.
Hickey, W.F., Vass, K., Lassmann, H., 1992. Bone marrow derived elements in the central nervous system: an immunohistochemical and ultrastructural survey of rat chimeras. J. Neuropathol. Exp. Neurol. 51, 246–256.
Honda, K., Yanai, H., Negishi, T., Asagiri, M., Sato, M., Mizutani, T., Shimada, N., Ohba, Y., Takaoka, A., Yoshida, N., Taniguchi, T., 2005a. IRF-7 is the master regulator of type-I interferon-dependent immune responses. Nature 434, 772–777.
Honda, K., Yanaai, H., Takaoka, A., Taniguchi, T., 2005b. Regulation of type I IFN induction: a current view. Int. Immunol. 17, 1367–1378.
Joly, E., Oldstone, M.B., 1992. Neuronal cells are deficient in loading peptidesonto MHC class I molecules. Neuron 8 (6), 1185–1190.
Johnston, C., Jiang, W., Chu, T., Levine, B., 2001. Identification of genes involved in host response to neurovirulent alphavirus infection. J. Virol. 75, 10431–10445.
Kajaste-Rudnitski, A., Mashimo, T., Frenkiel, M.P., Guénet, J.L., Lucas, M., Dèspres, P., 2006. The 2′-5′-oligoadenylate synthetase 1b is a potent inhibitor of West Nile Virus replication inside infected cells. J. Biol. Chem. 281 (8), 4624–4637.
Kim, K.I., Giannakopoulos, N.V., Virgin, H.W., Zhang, D.E., 2004. Interferon-inducible ubiquitin E2, Ubc8, is a conjugating enzyme for protein ISGylation. Mol. Cell Biol. 24 (21), 9592–9600.
Knapp, S., Yee, D.E., Frodsham, A.J., Hennig, B.J., Hellier, S., Zhang, L., Wright, M., Chiaramonte, M., Graves, M., Thomas, H.C., Hill, A.V., Thursz, M.R., 2003. Polymorphisms in interferon-induced genes and the outcome of hepatitis C virus infection: roles of MxA, OAS-1 and PKR. Genes Immun. 4 (411), 419.
Kurane, I., Innis, B.L., Nimmannitya, S., Nisalak, A., Rothman, A.L., Livingston, P.G., Janus, J., Ennis, F., 1990. Human immune responses to dengue viruses. Southeast Asian J. Trop. Med. Public Health 21, 658–662.
Lamb, J.R., Tugendreich, S., Hieter, P., 1995. Tetratrico peptide repeat interactions: to TPR or not to TPR? Trends Biochem. Sci. 20, 257–259.
Lenschow, D.J., Giannakopoulos, N.V., Gunn, L.J., Johnston, C., O'Guin, A.K., Schmidt, R.E., Levine, B., Virgin IV, H.W., 2005. Identification of interferon-stimulated gene 15 as an antiviral molecule during Sindbis virus infection in vivo. J. Virol. 79, 13974–13983.
Luplertlop, N., Missé, D., Bray, D., Deleuze, V., Gonzalez, J.P., Leardkamolkarn, V., Yssel, H., Veas, F., 2006. Dengue-virus-infected dendritic cells trigger vascular leakage through metalloproteinase overproduction. EMBO Rep. 7 (11), 1176–1181.
Malakhov, M.P., Malakhova, O.A., Kim, K.I., Ritchie, K.J., Zhang, D.E., 2002. UBP43 (USP18) specifically removes ISG15 from conjugated proteins. J. Biol. Chem. 277 (12), 9976–9981.
Malakhova, O.A., Kim, K.I., Luo, J.K., Zou, W., Kumar, K.G., Fuchs, S.Y., Shuai, K., Zhang, D.E., 2006. UBP43 is a novel regulator of interferon signaling independent of its ISG15 isopeptidase activity. EMBO J. 25 (11), 2368-2367.
Malathi, K., Dong, B., Gale Jr., M., Silverman, R.H., 2007. Small self-RNA generated by RNase L amplifies antiviral innate immunity. Nature, 448, 816–820.
Mehlhop, E., Diamond, M.S., 2006. Protective immune response against West Nile virus are primed by distinct complement activation pathways. J. Exp. Med. 203 (5), 1371–1381.
Meurs, E.F., Watanabe, Y., Kadereit, S., Barber, G.N., Katze, M.G., Chong, K., Williams, B.R., Hovanessian, A.G., 1992. Constitutive expression of human double-stranded RNA-activated p68 kinase in murine cells mediates phosphorilation of eukaryotic initiation factor 2 and partial resistance to encephalomyocarditis virus growth. J. Virol., 66 (10), 5804–5814.
Mishto, M., Bellavista, E., Santoro, A., Stolzing, A., Ligorio, C., Nacmias, B., Spazzafumo, L., Chiappelli, M., Licastro, F., Sorbi, S., Pession, A., Ohm, T., Grune, T., Franceschi, C., 2006. Immunproteasome and LMP2 polymorphism in aged and Alzheimer's disease brains. Neurobiol. Aging 27, 54–66.
Navarro-Sánchez, E., Desprès, P., Cedillo-Barrón, L., 2005. Innate immune responses to dengue virus. Arch. Med. Res. 36, 425–435.
Olson, J.K., Girvin, A.N., Miller, S.D., 2001. Direct activation of innate and antigen-presenting functions of microglia following infection with Theiler's virus. J. Virol. 75 (20), 9780–9789.
Pang, T., Cardosa, M.J., Guzman, M.G., 2007. Os cascades and perfect storms: the immunopathogenesis of dengue haemorrhagic fever-dengue shock syndrome. Immunol. Cell Biol. 85, 43–45.
Pasieka, J.T., Baas, T., Carter, S.V., Proll, C.S., Katze, G.M., Leib, A.D., 2006. Functional genomics analysis of herpes simplex virus type 1 counteraction of the host innate response. J. Virol. 80 (15), 7600–7612.
Perelygin, A.A., Scherbik, S.V., Zhulin, I.B., Stockman, B.M., Li, Y., Brinton, M.A., 2002. Positional cloning of the murine flavivirus resistance gene. Proc. Natl. Acad. Sci. U. S. A. 99 (14), 9322–9327.
Poersch, O.C., Pavoni, D.P., Queiroz, M.H., de Borba, L., Goldenberg, S., dos Santos, C.N., Krieger, M.A., 2005. Dengue virus infections: comparison of methods for diagnosing the acute disease. J. Clin. Virol. 32 (4), 272–277.
Redwine, J.M., Buchmeier, M.J., Evans, C.F., 2001. In vivo expression of major histocompatibility complex molecules on oligodendrocytes and neurons during viral infection. Am. J. Pathol. 159 (4), 1219–1224.
Rempel, L.A., Austin, K.J., Ritchie, K.J., Yan, M., Shen, M., Zhang, D.E., Henkes, L.E., Hansen, T.R., 2007. Ubp43 gene expression is required for normal Isg15 expression and fetal development. Reprod. Biol. Endocrinol. 5, 13.
Ritchie, K.J., Chang, S.H., Kim, K.I., Yan, M., Rosario, D., Li, L., de la Torre, J.C., Zhang, D.E., 2006. Role of ISG15 protease UBP43 (USP18) in innate immunity to viral infection. Nat. Med. 10 (12), 1374–1378.
Rothman, A.L., 2003. Immunology and immunopathogenesis of dengue disease. Adv. Virus Res. 60, 397–419.
Rothman, A.L., 2004. Dengue: defining protective versus pathologic immunity. J. Clin. Investig. 113 (7), 946–951.
Sariol, C.A., Muñoz-Jordán, J.L., Abel, K., Rosado, L.C., Pantoja, P., Giavedoni, L., Rodriguez, V., White, L.J., Martínez, M., Arana, T., Kraiselburd, E.N., 2007. Transcriptional activation of interferon-stimulated genes but not of cytokine genes after primary infection of Rhesus macaques with dengue virus type 1. Clin. Vacc. Immunol. 14 (6), 756–766.
Sarkar, S.N., Peters, G.A., Sen, G., 2005. Genes modulated by interferons and double-stranded RNA. In: Palese, P. (Ed.), Modulation of Host Gene Expression and Innate Immunity by Viruses. Springer, Norwell, MA, pp. 35–63.
Scherbik, S.V., Kluetzman, K., Perelygin, A.A., Brinton, M.A., 2007. Knock-in of the Oas1b^{r} allele into a flavivirus-induced disease susceptible mouse generates the resistant phenotype. Virology 368, 232–237.
Shaw, M.L., Palese, P., 2005. Viruses and the Innate Immune System. In: Palese, P. (Ed.), Modulation of Host Gene Expression and Innate Immunity by Viruses. Springer, Norwell, MA, pp. 1–9.
Shresta, S., Kyle, J.L., Snider, H.M., Basavapatna, M., Beatty, P.R., Harris, E., 2004. Interferon-dependent immunity is essential for resistance to primary dengue virus infection in mice, whereas T- and B-cell dependent immunity are less critical. J. Virol. 78 (6), 2701–2710.
Simmons, C.P., Popper, S., Dolocek, C., Chau, T.N.B., Grifiths, M., Dung, N.T.P., Long, T.H., Hoang, D.M., Chau, N.V., Thao, L.T.T., Hien, T.T., Relman, D.A., Farrar, J., 2007. Patterns of host genome-wide gene transcript abundance in the peripheral blood of patients with acute dengue hemorrhagic fever. J. Infect. Dis. 195 (7) 37409-1097-1107.
Smith, G.K., 2004. Linear models and empirical Bayes methods for assessing differential expression in microarray experiments. Stat. Appl. Genet. Mol. Biol. 3 (1) 3.
Streit, W.J., Graeber, M.B., Kreutzberg, G.W., 1989. Expression of Ia antigen on perivascular and microglial cells after sublethal and lethal motoneuron injury. Exp. Neurol. 105, 115–126.
SVS, Sistema de Vigilância Sanitária, Ministério da Saúde, Brasil, 2007. Balanço da Dengue, Janeiro-Julho de 2007. http://portal.saude.gov.br/portal/arquivos/pdf/dengue 0210.pdf.
Tusher, V.G., Tibshirani, R., Chu, G., 2001. Significance analysis of microarrays applied to the ionizing radiation response. Proc. Natl. Acad. Sci. U. S. A. 98 (9), 5116–5121.
Tumpey, T.M., Szretter, K.J., Van Hoeven, N., Katz, J.M., Kochs, G., Haller, O., García-Sastre, A., Staeheli, P., 2007. The Mx1 gene protects mice against the pandemic 1918 and highly lethal human H5N1 influenza virus. J. Virol. 81 (19), 10818–10821.
Van de Eynde, B.J., Morel, S., 2001. Differential processing of class-I-restricted epitopes by the standard proteasome and the immunoproteasome. Curr. Opin. Immunol. 13, 147–153.
Vass, K., Lassmann, H., 1990. Intrathecal application of interferon-gamma: progressive appearance of MHC antigens within the nervous system. Am. J. Pathol. 137, 789–800.
Venter, M., Myers, G.T., Wilson, A.M., Kindt, J.T., Paweska, T.J., Burt, J.F., Leman, A.P., Swanepoel, R., 2005. Gene expression in mice infected with West Nile virus strains of different neurovirulence. Virology 324, 119–140.
Warke, R.V., Xhaja, K., Martin, K.J., Fournier, M.F., Shan, S.K., Brizuela, N., de Bosch, N., Lapointe, D., Ennis, F.A., Rothman, A.L., Bosch, I., 2003. Dengue virus induces novel changes in gene expression of human umbilical vein endothelial cells. J. Virol. 77 (21), 11822–11832.
Warke, R.V., Martin, K.J., Giaya, K., Shaw, S.K., Rothman, A.L., Bosch, I., 2008. TRAIL is a novel antiviral protein against dengue virus. J. Virol. 82 (1), 555–564.
World Health Organization, 2002. WHO Fact Sheet 117. World Health Organization, Geneva, Switzerland.
Yang, J., Tugal, D., Reiss, C.S., 2006. The role of the proteasome-ubiquitin pathway in regulation of the IFN-γ mediated anti-VSV response in neurons. J. Neuroimmunol. 181, 34–45.
Yuan, W., Krug, R.M., 2001. Influenza B virus NS1 protein NS1 inhibits conjugation of the interferon (IFN)-induced ubiquitin-like ISG15 protein. EMBO J. 20, 362–371.